






Identification of Small-Molecule Inhibitors of Neutral Ceramidase (nCDase) via Target-Based High-Throughput Screening

SLAS Discovery
2021, Vol. 26(1) 113–121
© Society for Laboratory
Automation and Screening 2020
DOI: 10.1177/247255220945283
journals.sagepub.com/home/jbx


Yuka Otsuka¹, Michael V. Airola², Yong-Mi Choi², Nicolas Coant³ , Justin Snider³, Chris Cariello⁴, Essa M. Saied⁵ , Christoph Arenz⁶ , Thomas Bannister¹, Ron Rahaim Jr.¹, Yusuf A. Hannun^{2,3}, Justin Shumate¹, Louis Scampavia¹, John D. Haley^{3,4}, and Timothy P. Spicer¹ 

Abstract

There is interest in developing inhibitors of human neutral ceramidase (nCDase) because this enzyme plays a critical role in colon cancer. There are currently no potent or clinically effective inhibitors for nCDase reported to date, so we adapted a fluorescence-based enzyme activity method to a high-throughput screening format. We opted to use an assay whereby nCDase hydrolyzes the substrate RBM 14-16, and the addition of NaO₄ acts as an oxidant that releases umbelliferone, resulting in a fluorescent signal. As designed, test compounds that act as ceramidase inhibitors will prevent the hydrolysis of RBM 14-16, thereby decreasing fluorescence. This assay uses a 1536-well plate format with excitation in the blue spectrum of light energy, which could be a liability, so we incorporated a counterscreen that allows for rapid selection against fluorescence artifacts to minimize false-positive hits. The high-throughput screen of >650,000 small molecules found several lead series of hits. Multiple rounds of chemical optimization ensued with improved potency in terms of IC₅₀ and selectivity over counterscreen assays. This study describes the first large-scale high-throughput optical screening assay for nCDase inhibitors that has resulted in leads that are now being pursued in crystal docking studies and in vitro drug metabolism and pharmacokinetics (DMPK).

Keywords

HTS, colon cancer, neutral ceramidase, fluorescence, pharmacological inhibitors

Introduction

Colorectal cancer is the third most common cancer in the United States, with ~132,000 cases per year. Despite significant advances in early detection, progression to metastatic disease occurs in ~1/3 of patients, resulting in ~49,000 disease-related deaths.¹ Neutral ceramidase (nCDase) is highly expressed in colonic epithelium and converts ceramide to sphingosine. nCDase is a novel enzyme that displays no sequence or structural homology to other proteins.^{2,3} In intestinal tissues, nCDase is located at the brush border.⁴ The enzyme is tethered to the plasma membrane by a single-pass transmembrane helix and an extended highly glycosylated 60-amino acid linker. The large, glycosylated catalytic domain is attached to this linker and hydrolyzes dietary ceramide that is solubilized in bile acid micelles passing through the intestinal system.⁴ The ability of nCDase to hydrolyze ceramide in the outer leaflet of the plasma membrane is not known. nCDase is a lipid amidase and has no activity toward peptide bonds. Furthermore, the

substrate specificity has been well defined. nCDase is very specific for the endogenous stereoisomer of ceramide and

¹Department of Molecular Medicine, Scripps Research, The Scripps Research Molecular Screening Center, Jupiter, FL, USA

²Department of Biochemistry and Cell Biology, Stony Brook University, Stony Brook, NY, USA

³Stony Brook University Cancer Center, Stony Brook, NY, USA

⁴Department of Pathology, Stony Brook Renaissance School of Medicine, Stony Brook, NY, USA

⁵Chemistry Department, Faculty of Science, Suez Canal University, Ismailia, Egypt

⁶Institute for Chemistry, Humboldt Universität zu Berlin, Berlin, Germany

Received May 6, 2020, and in revised form June 18, 2020. Accepted for publication July 6, 2020.

Corresponding Author:

Timothy P. Spicer, Department of Molecular Medicine, Scripps Research, The Scripps Research Molecular Screening Center, Scripps Florida, 130 Scripps Way #1A1, Jupiter, FL 33458, USA.
Email: spicert@scripps.edu

cannot accommodate alterations to the terminal hydroxyl group of ceramide or alterations to the sphingoid backbone.^{5–7} The balance between pro-apoptotic ceramide and pro-proliferative sphingosine-1-phosphate (S1P) has emerged as a critical node in neoplastic transformation. Although nCDase has emerged as a therapeutic target, we currently lack pharmacological nCDase inhibitors for this unique lipid amidase suitable for *in vivo* studies.

nCDase is the one of the three families of ceramidases that are distinguished by their pH optima, subcellular localization, primary structure, mechanism, and function.⁸ The major ceramidase in intestinal tissues is nCDase.⁹ Ceramidases are lipid amidases that hydrolyze the amide bond of ceramide to generate sphingosine. In turn, sphingosine can be converted to S1P catalyzed by sphingosine kinases (SKs). Ceramide and S1P are bioactive lipids that are involved in the sphingolipid metabolism pathway. Sphingolipid metabolism is complex but summarized in several review articles.^{10–12} Sphingolipids are a family of membrane lipids that play an important role in transducing cellular signaling processes,^{10,13} including promoting migration, cell proliferation, senescence, and apoptosis. The defining chemical feature of sphingolipids is an amide bond, which is formed by the N-acetylation of the sphingoid base backbone to form ceramide. Ceramide and S1P are critical molecules in colon cancer development, promoting cell proliferation, survival, and angiogenesis.^{14–16} S1P has relatively low levels compared with other sphingolipids and acts through five distinct G-protein-coupled receptors (GPCRs). Redundancy in signaling between the five S1P receptors has impeded use of receptor antagonists for cancer indications. S1P is generated from sphingosine by sphingosine kinase 1 (SK1) in colon tissues.¹⁷ Critically, both SK1 and S1P are significantly elevated in colon cancer tissues compared with normal mucosal tissues in the azoxymethane-induced mouse model,¹⁷ and genetic deletion of SK1 can reduce the formation of aberrant crypt foci (ACFs) and progression to adenocarcinomas.¹⁸ Consistent with this, SK1 deletion in the APC-deficient mouse reduces adenoma formation.¹⁹ Importantly, 89% of human colon cancer samples demonstrated upregulation of SK1. Taken together, there is substantial evidence that increased SK1 and S1P levels contribute to colon carcinogenesis.

In contrast to the function of S1P, ceramide stimulates apoptosis, induces senescence, and inhibits cell proliferation. This is dependent on the stimulus, cell/tissue type, specific pathway of ceramide generation, and specific molecular species of ceramide.^{10,20–22} In the intestine, ceramide is generated by alkaline sphingomyelinase (alkSMase), which hydrolyzes dietary sphingomyelin (SM) to form ceramide and phosphoryl-choline.^{23,24} Ceramide is further metabolized by nCDase to form sphingosine.⁴ In human colon cancer tissue, there is a 50% reduction in ceramide levels compared with normal mucosa.²⁵ Interestingly, several

studies have looked at and found that dietary SM, which is converted to ceramide in the intestine, can inhibit colon cancer formation in animal models.^{26,27} Overall, the association between decreased ceramide levels and increased S1P levels implicates sphingolipid metabolism as a novel target for colon cancer therapy.⁹

Armed with this information, our strategy was to focus on the development of pharmacological inhibitors of nCDase with properties suitable for *in vivo* modeling, which is not possible with the current biochemical ceramidase inhibitors. The assay principle is based on the reaction between nCDase, a substrate, and sodium periodate (NaIO₄), which results in a fluorescent signal.²⁸ In order to perform large-scale screening, we miniaturized and optimized this assay to a 1536-well format. The assay was tested against 666,120 compounds from the Scripps Drug Discovery Library (SDDL) and the results are described herein.

Materials and Methods

Assay Reagents

Human nCDase was purified from Sf9 cells at Stony Brook University.²⁹ The assay used 0.5 µg/mL of nCDase in phosphate-buffered saline (PBS; Life Technologies, Carlsbad, CA). Final concentrations of 20 µM RBM 14–16 and sodium periodate (NaIO₄; Sigma, St. Louis, MO) were used as a substrate. Two types of buffers, reaction buffer and glycine buffer, were used in this assay. The reaction buffer contains 0.6% Triton-100 (Sigma), 150 mM NaCl (Sigma), and 25 mM phosphate (9.7 mM NaH₂PO₄ and 15.3 mM Na₂HPO₄; Sigma), and the pH was adjusted to 7.4. The glycine buffer contains 100 mM glycine (Sigma) and the pH was adjusted to 10.6. Sodium periodate (2.5 mg/mL; Sigma) was prepared fresh in glycine buffer on the day of the experiment. C6-urea-ceramide (Avanti, Polar Lipids, Alabaster, AL) was used as a pharmacological control for the high-throughput screening (HTS) campaign.

Compounds

The SDDL currently consists of 666,120 compounds, representing a diversity of druglike compound scaffolds targeted to traditional and nontraditional drug discovery biological targets. The SDDL has been curated from more than 20 commercial and academic sources and contains more than 40,000 compounds unique to Scripps. It is important to note that the SDDL also has minimum overlap (<14%) with any other known large compound library. The SDDL compounds were selected based on scaffold novelty, physical properties, and spatial connectivity. By design, the diversity of the SDDL mimics that of much larger collections found at major pharmaceutical companies yet is responsive to lessons learned from successful drug discovery efforts and

emerging trends in HTS library construction.^{30–34} In its current state, the SDDL has several focused sublibraries for screening popular drug discovery target classes (e.g., kinases/transferases, GPCRs, ion channels, nuclear receptors, hydrolases, transporters, and structure–activity relationships [SARs]), as well as diverse chemistries (e.g., click chemistry, PAINS-free, Fsp3 enriched, and natural product collections) and those based on physical properties (“rule of five,” “rule of three,” polar surface area, etc.).

A 1536-Well Assay protocol

This assay is performed by incubating 2 μL /well of nCDase (final concentration: 0.5 $\mu\text{g}/\text{mL}$ in PBS) with 50 nL/well compound and 2 μL /well RBM 14-16 (final concentration: 20 μM in reaction buffer) for 3 h at 37 $^{\circ}\text{C}$. This is followed by the addition of 2 μL /well sodium periodate (NaIO_4 in glycine buffer) and centrifugation (1000 RPM for 5 min), followed by the measurement of fluorescence using the PerkinElmer ViewLux (excitation 360 nm; emission 460 nm). Ceramidase hydrolyzes RBM 14-16, and the addition of NaIO_4 acts as an oxidant that releases umbelliferone, resulting in a fluorescent signal. As designed, test compounds that act as nCDase inhibitors will prevent the hydrolysis of RBM 14-16, thereby decreasing well fluorescence.

Data Acquisition and Analysis

Raw assay data were imported into the Scripps corporate database and subsequently analyzed using Symyx software. The activity of each compound was calculated on a per-plate basis using the following equation:

$$\text{Percent inhibition of compound} = 100 \times \left(\frac{\text{Test well} - \text{Median low control}}{\text{Median high control} - \text{Median low control}} \right) \quad (1)$$

where “high control” represents wells containing DMSO and substrate (RBM 14-16) and “low control” represents wells containing DMSO, substrate (RBM 14-16), and nCDase. The assay robustness was calculated on a per-plate basis using Z' analysis generated using the high and low controls ($N = 24$ each per plate). Each plate must have scored a Z' of >0.5 in order to be accepted for further analysis. If not, it was rescheduled and tested until we achieved the proper Z' .³⁵ A mathematical algorithm was used to determine active compounds, which we refer to as an interval-based hit cutoff, which allows us to retain more hits than when we use a standard hit cutoff. Four values were calculated: (1) the average percent inhibition of all high controls tested plus three times the standard deviation of the high controls, (2) the average percent inhibition of all low controls tested minus three times the standard deviation of

the low controls, (3) the average percent inhibition of all compounds tested between values 1 and 2, and (4) three times their standard deviation. The sum of two of these values, 3 and 4, was used as a cutoff parameter; that is, any compound that exhibited greater percent inhibition than the cutoff parameter was declared active and that percent inhibition value is referred to as the “hit cutoff.”

Counterscreen

To identify compounds that may act as quenchers or artifacts that optically interfere with fluorescence, a counterscreen was performed. For this screen, a “post-assay-pinning” method was employed. This assay was performed in format similar to that of the nCDase inhibitory assay, but compounds were transferred after the addition of NaIO_4 .

Secondary and Tertiary nCDase Assays

Two assays were used to further validate HTS hits and further remove fluorescence interfering compounds from consideration. C12-NBD-ceramide (Cayman Chemical, Ann Arbor, MI) was used as a fluorescent nCDase substrate and reaction products were separated by reverse-phase high-performance liquid chromatography (HPLC). The reaction conditions were 20 μM substrate, 1 nM nCDase in 75 mM NaCl, 25 mM HEPES (pH 8.0), and 0.4% Triton X-100, for 2 h at 37 $^{\circ}\text{C}$ in a final volume of 100 μL . Samples were extracted with 1:1 chloroform-methanol (Sigma), dried under nitrogen gas, and resuspended in 60 μL of HPLC mobile phase B. Reaction products were separated by reverse-phase HPLC using a Spectra 3 μm C8SR column (3 μm particle, 3.0 \times 150 mm; Peeke Scientific, Novato, CA). Mobile phase A contained 0.2% formic acid and 1 mM ammonium formate in HPLC-grade water (Sigma). Mobile phase B contained 0.2% formic acid (Fisher Scientific, Hanover Park, IL) and 1 mM ammonium formate (Sigma) in HPLC-grade methanol (Sigma). All enzyme assays were technically and experimentally duplicated. A Förster resonance energy transfer (FRET)-based assay³⁶ was performed using 20 μM substrate ES.173.cds,³⁶ 50 ng of nCDase, 75 mM NaCl, 15 mM sodium phosphate (pH 7.4), and 0.3% Triton X-100 for 3 h in 96 black well plates. The excitation wavelength was 347 nm, the emission was measured at 430 nm and 530 nm, and a ratio of 430/530 nm was generated.

Results

The 96-well format nCDase inhibitor fluorescence assay^{28,37} was miniaturized and optimized in the 1536-well format for HTS. The modification of assay conditions, including incubation times and reagent concentrations, was based on increasing the Z' value and reproducibility of the assay. The K_m (Michaelis constant) of this assay for its substrate is 0.84

Table 1. Summary of the nCDase Inhibitor HTS Campaign.

	Screen Type	Readout	Number of Compounds Tested	Selected Criteria	Number of Selected Compounds (% Hit Rate)	Z'	S/B
1	Primary	Fluorescent	666,120	Plate based interval	2499 (0.38)	0.93 ± 0.04	36.23 ± 11.27
2a	Confirmation	Fluorescent	2497	5.64% (DMSO: avg + 3SD)	125 (5.01)	0.94 ± 0.02	45.38 ± 0.25
2b	Counterscreen	Fluorescent	2497	4.50% (DMSO: avg + 3SD)	20 (0.80)	0.97 ± 0.002	46.19 ± 0.26
3a	Titration	Fluorescent	122	$IC_{50} < 10 \mu\text{M}$	1 (0.81)	0.85 ± 0.007	45.38 ± 0.36
3b	Counterscreen titration	Fluorescent	122	$IC_{50} < 10 \mu\text{M}$	0 (0)	0.94 ± 0.03	42.13 ± 0.44

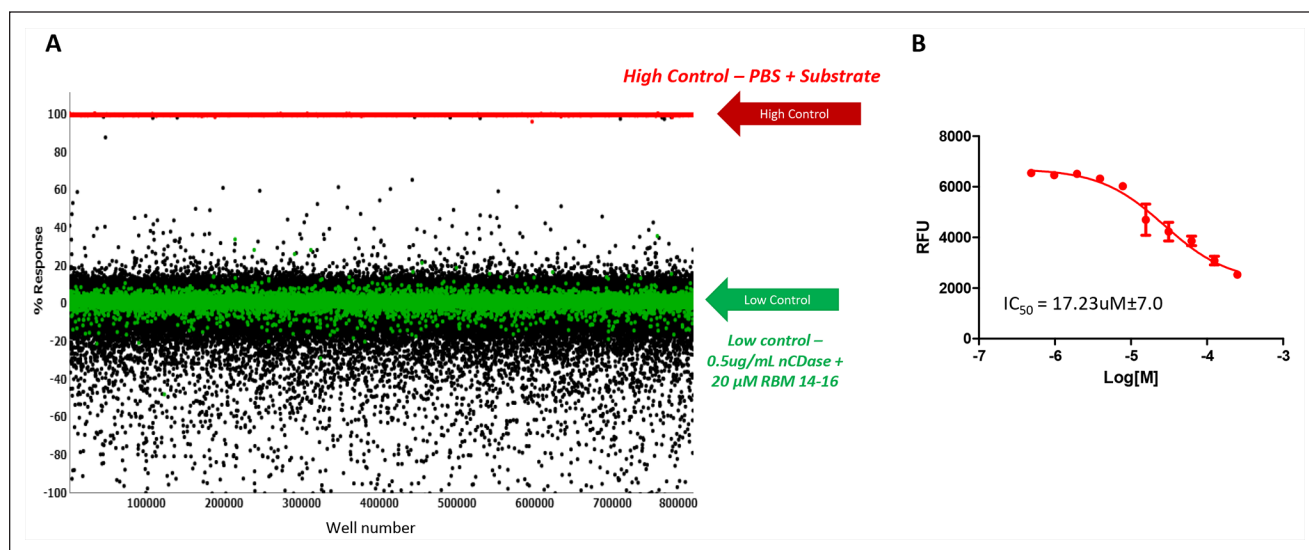


Figure 1. (A) Scatterplot of data from nCDase inhibitor primary HTS. Each dot graphed represents the activity result of a well containing test compound (black dots) or control (red and green dots). (B) Titration result of the pharmacological control compound, C6-urea-ceramide. $N = 5$ separate experiments, $N = 4$ wells per replicate point, error bars are shown. The average calculated IC_{50} was $17.23 \pm 7.0 \mu\text{M}$.

mol%. The assay kinetics were linear with respect to time ($r^2 = 0.96$) and enzyme concentration ($r^2 = 0.99$). The enzyme was found to be stable for 1 week at room temperature. During the 1536-well implementation, most changes to the 96-well format were well tolerated, but we observed two issues that we overcame. The first was that the NaIO_4 was perceived to quench the enzyme turnover. However, this was not the case and the assay proceeded even after its addition. The solution was to automate the assay completely, which essentially controlled for the exact timing for each step in the protocol, especially considering the endpoint read. We also observed bubble formation after adding NaIO_4 . This caused excessive variability in the fluorescent reads on a well-to-well basis, which we ameliorated using an angle solenoid valve tip dispense with reduced pressure (10 psi to 6 psi) to

allow for gentler addition of the reagent to all wells. We also implemented centrifugation after addition of NaIO_4 . Both steps afforded us with excellent well-to-well uniformity.

The first step of the HTS campaign was screening the nCDase inhibitor fluorescence assay against the 666,120 compounds of the SDDL. In this primary screen, compounds were tested at a single concentration in singlicate at a final nominal concentration of $17.4 \mu\text{M}$. Assay performance was excellent, with an average Z' of 0.93 ± 0.04 and an average signal-to-background ratio (S/B) of 36.23 ± 11.27 ($n = 536$ plates). A summary of the results of the primary screening assay is shown in **Table 1** and **Figure 1**. The ceramidase C6-urea-ceramide inhibitor was used as a pharmacological control for the assay, and the primary screen yielded an IC_{50} value of $17.23 \pm 7.0 \mu\text{M}$, which was

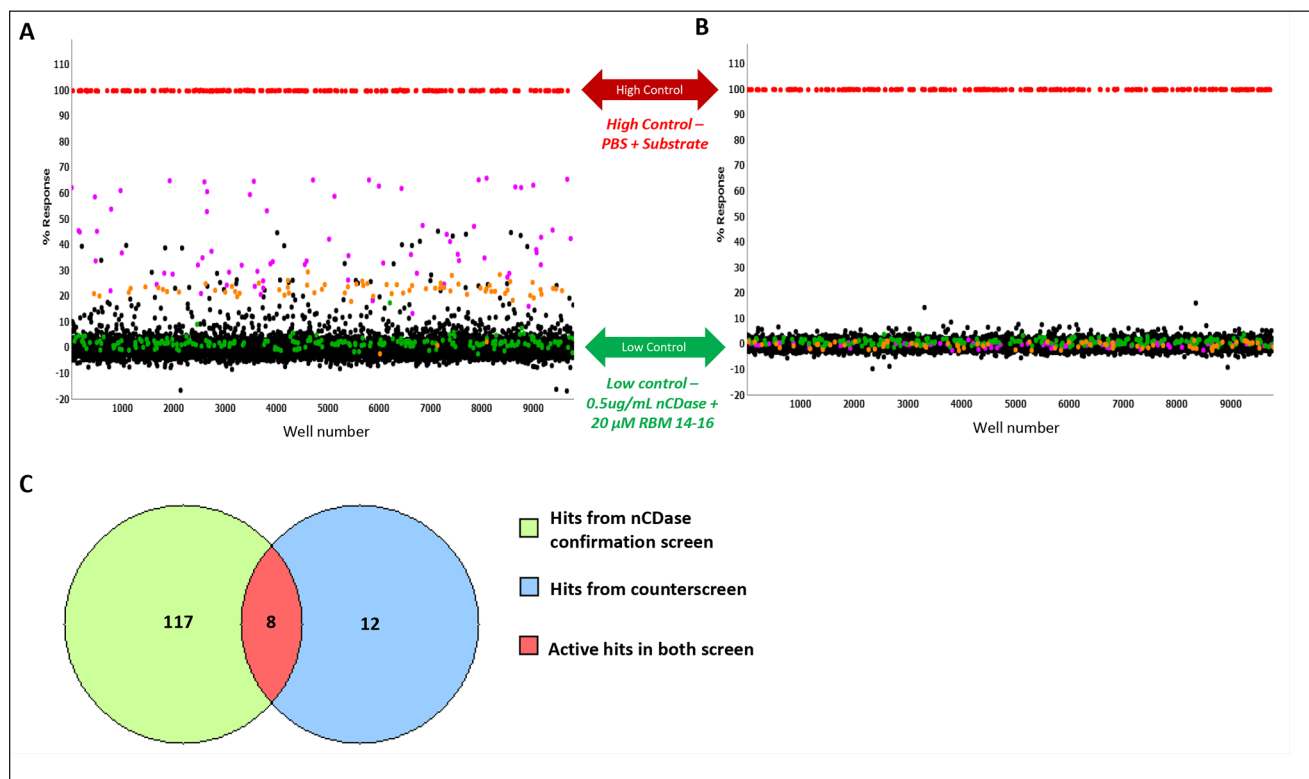


Figure 2. (A,B) The scatterplots of data from confirmation and counterscreen. Each dot graphed represents the activity result of a well containing test compound (black dots) or control (red and green for high and low controls, respectively). The red dotted lines represent the hit cutoff percentage. (A) Confirmation screen. (B) Counterscreen. (C) Venn diagram of compounds found active in the confirmation and counterscreen. Of the 2497 compounds tested, 125 compounds confirmed activity and 117 appear to be selective/active in the confirmation screen and inactive in the counterscreen assay.

an expected range. A plate-based interval cutoff was used to identify active compounds, and the primary screen yielded 2499 hits (hit rate: 0.38%). From the list of hits, 2497 compounds were available to test in the confirmation screen.

After completion of cherry-picking of the selected compounds, the confirmation screen was run. This assay utilized the same reagents and detection system as the primary screen, but the selected compounds were tested at a nominal concentration of 17.4 μM , in triplicate. The confirmation assay performance yielded an average Z' of 0.94 ± 0.02 and an S/B of 45.38 ± 0.25 ($n = 12$ plates) (Fig. 2A, Table 1). Using a hit cutoff of 5.64% inhibition (standard cutoff: average + $3 \times \text{SD}$ of all wells treated with vehicle only; $N = 5120$), 125 hits confirmed their activity (hit rate: 5.01%) (Table 1). To identify compounds that optically interfered with fluorescence measurements, the counterscreen assay was also performed in parallel with the exact same compounds. The fluorescence interference counterscreen or “post-assay-pinning” counterscreen assay performance was excellent, with an average Z' of 0.97 ± 0.002 and an S/B of 49.19 ± 0.26 (Table 1). This counterscreen yielded 20 hits with a 3.85% hit cutoff parameter (standard cutoff of DMSO plate) (Fig. 2B). A Venn diagram representing which compounds were determined to be active in

each assay is shown Figure 2C. One hundred seventeen compounds appear to be active only in the nCDase confirmation assay. So as not to rule out any inhibitor too early, we chose to pursue all 125 confirmed actives. One hundred twenty-two compounds out of 125 hits from the confirmation assay were available and tested in a titration assay.

For the titration assay, each of the 122 compounds was tested as 10-point dose–response titrations (threefold dilutions) in triplicate. The nCDase inhibitor titration assay performance was consistent, with an average Z' of 0.85 ± 0.007 and an S/B of 45.38 ± 0.36 (Table 1). For each test compound, the percent inhibition was plotted against the compound concentration. A four-parameter equation describing a sigmoidal dose–response curve was then fitted with an adjustable baseline using Assay Explorer software (Symyx Technologies Inc.). The reported IC_{50} values were generated from fitted curves by solving for the X -intercept value at the 50% activation level of the Y -intercept value. The following rule was used to declare a compound as “active” or “inactive”: compounds with no response were considered inactive. For this assay, 49 compounds had a response of $>50\%$ and 4 compounds and one analog showed high activity with an IC_{50} of $<10 \mu\text{M}$ (Fig. 3). The counterscreen titration assay was also performed in parallel,

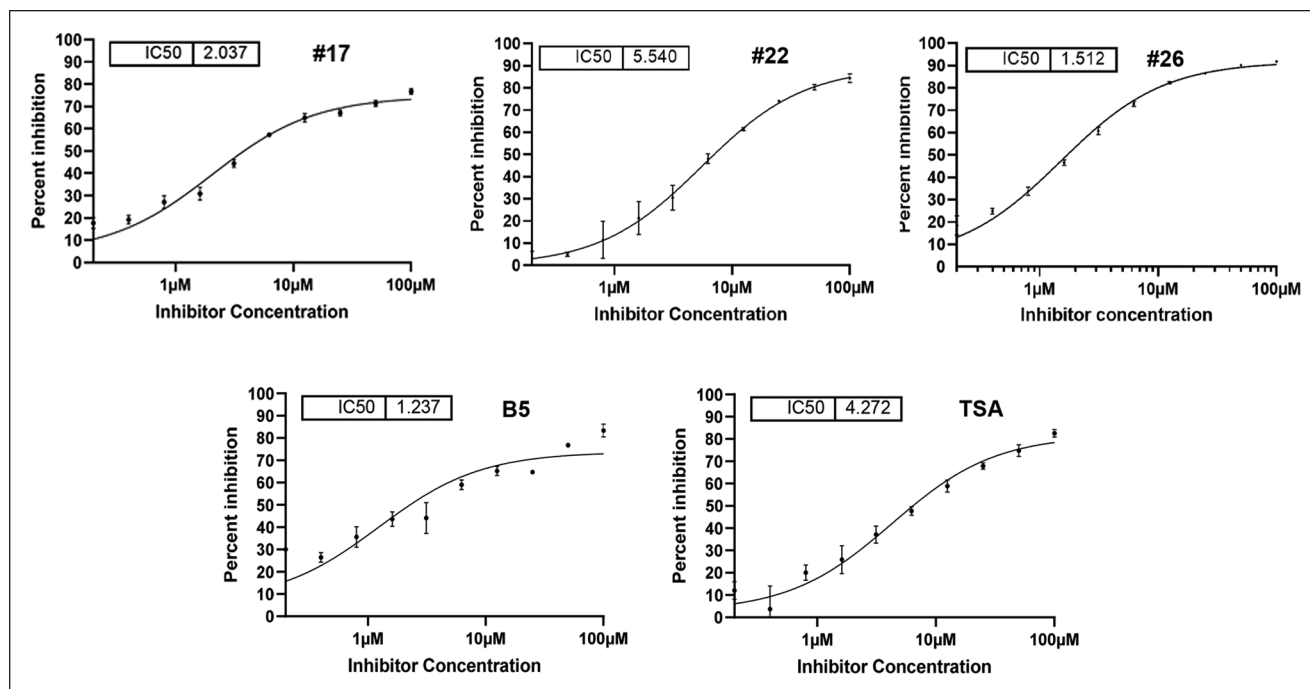


Figure 3. Active compound potency and efficacy. Active compounds from screening (17, 22, and B5; control TSA) and an analog of compound 22 (compound 26) were dose titrated using the RBM-ceramide assay to establish IC₅₀ potency and percent maximal inhibition efficacy. The IC₅₀ is shown in micromolar concentration for each.

and the assay statistics were consistent, with an average Z' of 0.94 ± 0.03 and an S/B of 42.13 ± 0.44 (Table 1). There was no compound found that had an IC₅₀ of $<10 \mu\text{M}$ in this counterscreen assay.

Following the HTS campaign, the four analogs were expanded on via medicinal chemistry approaches to select for modifications that retain favorable druglike properties (compliant with rule of five) and are also anticipated to contribute a meaningful direction to SAR. Fresh powders of the initial analogs as well as expansion set were either obtained from chemical vendors or synthesized in-house. Hit validation was performed by comparison of manual RBM-ceramide, FRET ceramide, and NBD-ceramide-HPLC assays. FRET ceramide and NBD-ceramide-HPLC assays were included to overcome the sensitivity of the RBM-ceramide assay to compound fluorescence. In total, 678 compounds and analogs were selected from the RBM HTS assay and DOCK screening, which was performed using the crystal structure of nCDase and predicted binding pose of ceramide within the active site. These selected compounds and analogs were screened at a fixed dose (435 compounds) or full 10-point IC₅₀ (243 compounds). Twenty-two compounds were prioritized with an IC₅₀ of $<50 \mu\text{M}$ and percent inhibition of >70 . Five chemical compound classes were identified with an IC₅₀ of $<20 \mu\text{M}$. Several series were selected for further characterization using RBM-ceramide, FRET, and NBD-ceramide HPLC assays: manual RBM-ceramide assays were performed

with fresh compounds showing IC₅₀ values in the low micromolar range. Trichostatin A (TSA), a class I HDAC inhibitor, was identified in pilot screening and has served as a benchmark compound showing an IC₅₀ value of $4 \mu\text{M}$, while for comparison C6-urea-ceramide typically shows IC₅₀ values of $\sim 20 \mu\text{M}$ (data not shown). Screening hits 17, 22, and B5 showed IC₅₀ values ranging from 1 to $6 \mu\text{M}$. A close analog of compound 22, compound 26 showed improved potency with an IC₅₀ of $1.5 \mu\text{M}$. These data are shown in Figure 3.

Compounds 17 and 22 were further tested using FRET probes for ceramidases³⁶ using C6-urea as a positive control. Two doses were tested with maximal activity at $30 \mu\text{M}$. Compounds 17 and 22 showed nCDase inhibitions of $\sim 67\%$ and 88% , respectively (Fig. 4A).

The NBD-ceramide follow-up assay was performed to further validate test compounds and remove potential fluorescence interference. Initial NBD-ceramide assays on 22 HTS hits (data not shown) prioritized compounds 17 and 22. IC₅₀ determinations on compounds 17, 26 (a compound 22 analog), and B5 were performed using TSA as a positive control. IC₅₀ values of $<10 \mu\text{M}$ were observed, with compound 26 showing a best potency with an IC₅₀ of $1.6 \mu\text{M}$ (Fig. 4B).

Discussion

In this study, we applied large-scale HTS to find pharmacological inhibitors of nCDase, which is a therapeutic target

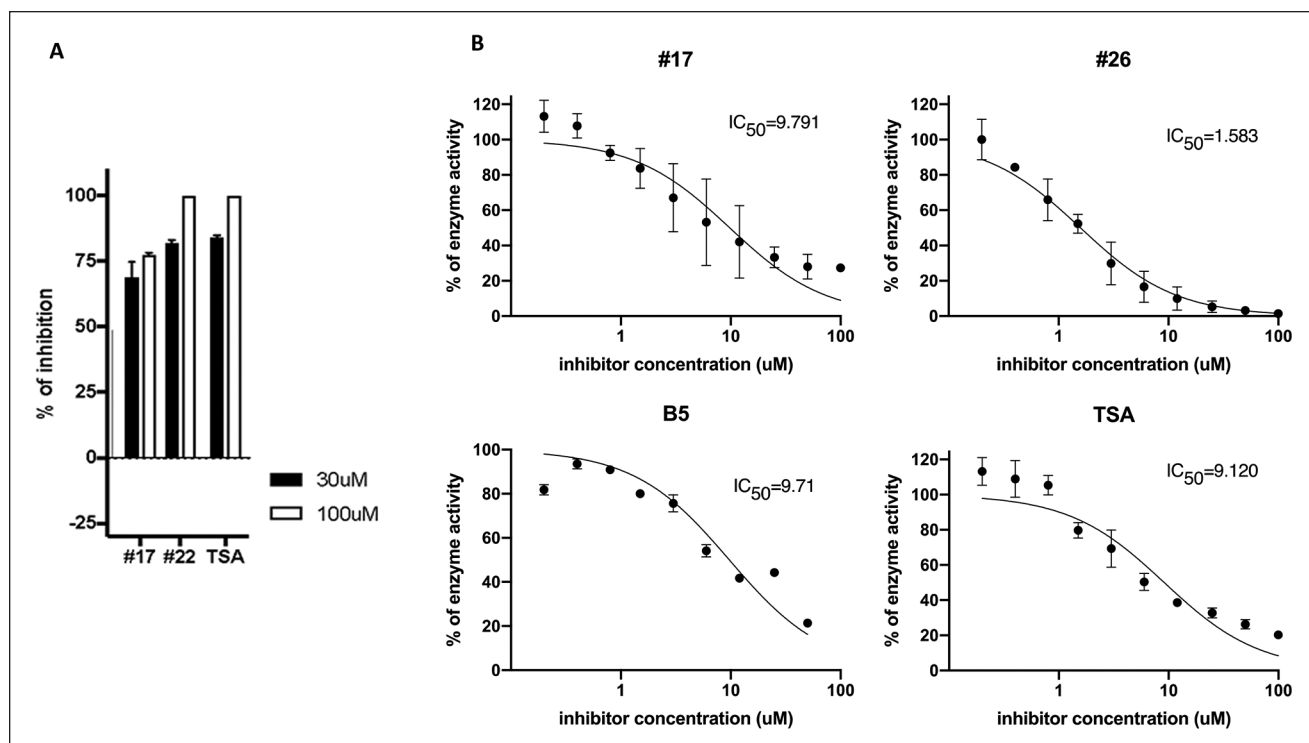


Figure 4. Confirmation of active compound potency and efficacy using orthogonal FRET and NBD-ceramide HPLC assays. **(A)** FRET assay confirmation of prioritized compound series 17 and 26 with TSA control reference compound identified in pilot HTS screening. **(B)** NBD-ceramide HPLC dose titration confirmation of compounds 17, 26, and B5 and the TSA control. HPLC separation of fluorescent substrate, product, and test compound based on retention time removes potential compound fluorescent interference. The IC₅₀ is shown in micromolar concentration for each.

for colorectal cancer. The primary screen against 666,120 compounds from SDDL resulted in 2499 hits with great plate statistics. The hit rate for this screening was 0.38%, which is in line with expectations based on pilot screening initiatives and the active site of the enzyme, which is somewhat predicted to be difficult to target.

The crystal structure of nCDase has revealed that the active site is accessed via a ~20 Å hydrophobic channel with more polar lipid head group interactions in the base of the active site.²⁹ The hydrophobic channel provides an interaction surface holding ceramide in place for cleavage and release of the sphingoid tail. Active site chemical inhibitors need to be able to traverse the channel and make more electrostatic head group interactions at the catalytic site. On this basis, a relatively low hit rate was predicted.

From the 2497 compounds, we further narrowed them down to 49 compounds that showed a response of >50% in the titration assay, and of those, 4 compounds had an IC₅₀ of <10 μM. All the assays were performed with exceptionally good Z' scores (Table 1), providing robustness in the outcomes.

In order to obtain optimum assay conditions in the 1536-well format, we tested multiple variables, including plate type, titration of nCDase and substrates, and adjustment in incubation times. The timing for reading after the addition

of NaO₄ was modified once we learned that the reaction between nCDase and substrate (RBM 14-16) did not stop after the addition of NaO₄. The addition of NaO₄ also caused bubble formation that resulted in decreased well fluorescence, and thus caused a false positive. This problem was resolved by using an angled tip for dispensing NaO₄ and increasing the speed of centrifugation after addition.

For each assay, as a pharmacological inhibitor control, we used C6-urea-ceramide, which is a unique ceramide-based inhibitor⁷ and the first specific inhibitor of nCDase.³⁸ However C6-urea-ceramide is an unstable molecule and lost its activity about 1 month later, which forced re-creation of fresh source plates using C6-urea-ceramide obtained as powder. This is something to keep in mind for longer HTS campaigns. In follow-up assays, we moved to TSA as a more stable and potent positive control.

In this HTS campaign, we used “post-assay-pinning” as counterscreening, which eliminated false positives caused by compound interference. To further validate and characterize compound potency and efficacy, we performed secondary FRET-based and tertiary NBD-ceramide HPLC separation-based confirmation assays. These assays confirm the findings of the HTS campaign. We have identified several chemical classes with potency ranges of 1–10 μM

and maximal percent inhibitions of 70%–95%. Initial SAR relationships have been observed and further compound class and singleton analogs are being evaluated. Diverse, active compounds will be used for co-crystal studies to inform chemical optimization.

In summary, we have thus far identified and confirmed multiple active compound classes using the HTS strategy described. Chemical optimization, pharmacokinetic evaluation, and biological characterization efforts are underway.

Acknowledgments

We thank Pierre Baillargeon and Lina DeLuca (Scripps Florida) for compound management. We thank Michael Simoes and Amalia Saleh (Stony Brook University) for assisting with follow-up compound evaluation. This work was supported using the ChemAxon software tools which have been provided free of charge.

Declaration of Conflicting Interests


The authors declared no potential conflicts of interest with respect to the research, authorship, and/or publication of this article.

Funding

The authors disclosed receipt of the following financial support for the research, authorship, and/or publication of this article: The studies were funded by the Stony Brook Cancer Center and by the National Cancer Institute (R01CA221948) as part of a joint collaboration between Scripps Florida and Stony Brook University Cancer Center.

ORCID iDs

Nicolas Coant  <https://orcid.org/0000-0001-9237-2132>

Essa M. Saied  <https://orcid.org/0000-0002-7342-6200>

Christoph Arenz  <https://orcid.org/0000-0001-7613-9437>

Timothy P. Spicer  <https://orcid.org/0000-0002-9080-4226>

References

- American Cancer Society. Cancer Facts & Figures 2016. <https://www.cancer.org/research/cancer-facts-statistics/all-cancer-facts-figures/cancer-facts-figures-2016.html> (accessed July 15, 2020).
- Mao, C.; Obeid, L. M. Ceramidases: Regulators of Cellular Responses Mediated by Ceramide, Sphingosine, and Sphingosine-1-Phosphate. *Biochim. Biophys. Acta* **2008**, *1781*, 424–434.
- El Bawab, S.; Roddy, P.; Qian, T.; et al. Molecular Cloning and Characterization of a Human Mitochondrial Ceramidase. *J. Biol. Chem.* **2000**, *275*, 21508–21513.
- Selzner, M.; Bielawska, A.; Morse, M. A.; et al. Induction of Apoptotic Cell Death and Prevention of Tumor Growth by Ceramide Analogues in Metastatic Human Colon Cancer. *Cancer Res.* **2001**, *61*, 1233–1240.
- Galadari, S.; Wu, B. X.; Mao, C.; et al. Identification of a Novel Amidase Motif in Neutral Ceramidase. *Biochem. J.* **2006**, *393*, 687–695.
- El Bawab, S.; Bielawska, A.; Hannun, Y. A. Purification and Characterization of a Membrane-Bound Nonlysosomal Ceramidase from Rat Brain. *J. Biol. Chem.* **1999**, *274*, 27948–27955.
- El Bawab, S.; Usta, J.; Roddy, P.; et al. Substrate Specificity of Rat Brain Ceramidase. *J. Lipid Res.* **2002**, *43*, 141–148.
- Foss, F. W., Jr.; Mathews, T. P.; Kharel, Y.; et al. Synthesis and Biological Evaluation of Sphingosine Kinase Substrates as Sphingosine-1-Phosphate Receptor Prodrugs. *Bioorg. Med. Chem.* **2009**, *17*, 6123–6136.
- Garcia-Barros, M.; Coant, N.; Kawamori, T.; et al. Role of Neutral Ceramidase in Colon Cancer. *FASEB J.* **2016**, *30*, 4159–4171.
- Li, F.; Zhang, N. Ceramide: Therapeutic Potential in Combination Therapy for Cancer Treatment. *Curr. Drug Metab.* **2015**, *17*, 37–51.
- Hannun, Y. A.; Obeid, L. M. Many Ceramides. *J. Biol. Chem.* **2011**, *286*, 27855–27862.
- Maceyka, M.; Milstien, S.; Spiegel, S. Sphingosine-1-Phosphate: The Swiss Army Knife of Sphingolipid Signaling. *J. Lipid Res.* **2009**, *50* (Suppl), S272–S276.
- Airola, M. V.; Hannun, Y. A. Sphingolipid Metabolism and Neutral Sphingomyelinases. *Handb. Exp. Pharmacol.* **2013**, *215*, 57–76.
- Taha, T. A.; Argraves, K. M.; Obeid, L. M. Sphingosine-1-Phosphate Receptors: Receptor Specificity versus Functional Redundancy. *Biochim. Biophys. Acta* **2004**, *1682*, 48–55.
- Taha, T. A.; Hannun, Y. A.; Obeid, L. M. Sphingosine Kinase: Biochemical and Cellular Regulation and Role in Disease. *J. Biochem. Mol. Biol.* **2006**, *39*, 113–131.
- Kawamori, T.; Osta, W.; Johnson, K. R.; et al. Sphingosine Kinase 1 Is Up-Regulated in Colon Carcinogenesis. *FASEB J.* **2006**, *20*, 386–388.
- Kawamori, T.; Kaneshiro, T.; Okumura, M.; et al. Role for Sphingosine Kinase 1 in Colon Carcinogenesis. *FASEB J.* **2009**, *23*, 405–414.
- Kohno, M.; Momoi, M.; Oo, M. L.; et al. Intracellular Role for Sphingosine Kinase 1 in Intestinal Adenoma Cell Proliferation. *Mol. Cell. Biol.* **2006**, *26*, 7211–7223.
- Deng, X.; Yin, X.; Allan, R.; et al. Ceramide Biogenesis Is Required for Radiation-Induced Apoptosis in the Germ Line of *C. elegans*. *Science* **2008**, *322*, 110–115.
- Mullen, T. D.; Jenkins, R. W.; Clarke, C. J.; et al. Ceramide Synthase-Dependent Ceramide Generation and Programmed Cell Death: Involvement of Salvage Pathway in Regulating Postmitochondrial Events. *J. Biol. Chem.* **2011**, *286*, 15929–15942.
- Pettus, B. J.; Chalfant, C. E.; Hannun, Y. A. Ceramide in Apoptosis: An Overview and Current Perspectives. *Biochim. Biophys. Acta* **2002**, *1585*, 114–125.
- Duan, R. D.; Bergman, T.; Xu, N.; et al. Identification of Human Intestinal Alkaline Sphingomyelinase as a Novel Ecto-Enzyme Related to the Nucleotide Phosphodiesterase Family. *J. Biol. Chem.* **2003**, *278*, 38528–38536.
- Duan, R. D.; Hertervig, E.; Nyberg, L.; et al. Distribution of Alkaline Sphingomyelinase Activity in Human Beings and Animals. Tissue and Species Differences. *Dig. Dis. Sci.* **1996**, *41*, 1801–1806.

24. Kono, M.; Dreier, J. L.; Ellis, J. M.; et al. Neutral Ceramidase Encoded by the *Asah2* Gene Is Essential for the Intestinal Degradation of Sphingolipids. *J. Biol. Chem.* **2006**, *281*, 7324–7331.
25. Dillehay, D. L.; Webb, S. K.; Schmelz, E. M.; et al. Dietary Sphingomyelin Inhibits 1,2-Dimethylhydrazine-Induced Colon Cancer in CF1 Mice. *J. Nutr.* **1994**, *124*, 615–620.
26. Mazzei, J. C.; Zhou, H.; Brayfield, B. P.; et al. Suppression of Intestinal Inflammation and Inflammation-Driven Colon Cancer in Mice by Dietary Sphingomyelin: Importance of Peroxisome Proliferator-Activated Receptor Gamma Expression. *J. Nutr. Biochem.* **2011**, *22*, 1160–1171.
27. Garcia-Barros, M.; Coant, N.; Truman, J. P.; et al. Sphingolipids in Colon Cancer. *Biochim. Biophys. Acta* **2014**, *1841*, 773–782.
28. Bedia, C.; Camacho, L.; Abad, J. L.; et al. A Simple Fluorogenic Method for Determination of Acid Ceramidase Activity and Diagnosis of Farber Disease. *J. Lipid Res.* **2010**, *51*, 3542–3547.
29. Airola, M. V.; Allen, W. J.; Pulkoski-Gross, M. J.; et al. Structural Basis for Ceramide Recognition and Hydrolysis by Human Neutral Ceramidase. *Structure* **2015**, *23*, 1482–1491.
30. Leeson, P. D.; Springthorpe, B. The Influence of Drug-Like Concepts on Decision-Making in Medicinal Chemistry. *Nat. Rev. Drug Discov.* **2007**, *6*, 881–890.
31. Axerio-Cilies, P.; Castaneda, I. P.; Mirza, A.; et al. Investigation of the Incidence of “Undesirable” Molecular Moieties for High-Throughput Screening Compound Libraries in Marketed Drug Compounds. *Eur. J. Med. Chem.* **2009**, *44*, 1128–1134.
32. Harvey, A. L. Natural Products in Drug Discovery. *Drug Discov. Today* **2008**, *13*, 894–901.
33. Potashman, M. H.; Duggan, M. E. Covalent Modifiers: An Orthogonal Approach to Drug Design. *J. Med. Chem.* **2009**, *52*, 1231–1246.
34. Baell, J. B.; Holloway, G. A. New Substructure Filters for Removal of Pan Assay Interference Compounds (PAINS) from Screening Libraries and for their Exclusion in Bioassays. *J. Med. Chem.* **2010**, *53*, 2719–2740.
35. Zhang, J. H.; Chung, T. D.; Oldenburg, K. R. A Simple Statistical Parameter for Use in Evaluation and Validation of High Throughput Screening Assays. *J. Biomol. Screen.* **1999**, *4*, 67–73.
36. Mohamed, Z. H.; Rhein, C.; Saied, E. M.; et al. FRET Probes for Measuring Sphingolipid Metabolizing Enzyme Activity. *Chem. Phys. Lipids* **2018**, *216*, 152–161.
37. Bedia, C.; Casas, J.; Garcia, V.; et al. Synthesis of a Novel Ceramide Analogue and Its Use in a High-Throughput Fluorogenic Assay for Ceramidases. *Chembiochem* **2007**, *8*, 642–648.
38. Usta, J.; El Bawab, S.; Roddy, P.; et al. Structural Requirements of Ceramide and Sphingosine Based Inhibitors of Mitochondrial Ceramidase. *Biochemistry* **2001**, *40*, 9657–9668.